# Influence of the dynamics of fluctuations in a magnetic material in the vicinity of the Curie point on the kinetics of surface growth of new-phase islands

V. D. Borman, E. P. Gusev, Yu. Yu. Lebedinskiĭ, A. P. Popov, and V. I. Troyan

*Engineering-Physics Institute, Moscow*

(Submitted 21 July, 1988)
Zh. Eksp. Teor. Fiz. **95**, 1378–1391 (April 1989)

The rate of formation of submonolayer oxide-phase islands on the surface of nickel has been studied experimentally over a wide range of temperatures, including the Curie point $T_C$. Anomalous behavior of the rate of formation of the oxide phase was observed in the vicinity of $T_C$. The experimental results are described on the basis of a proposed mechanism of oxide phase island growth and a theory of activated processes on the surface of a magnetic material in the vicinity of $T_C$.

## I. INTRODUCTION

In an earlier paper[1] we pointed out that the dynamics of fluctuations of the magnetic moment of a magnetic material, which appear in the vicinity of a second-order phase transition in the interior of a solid, can influence the kinetics of nonequilibrium activated processes on the surface. It follows from Ref. 1 that an increase in the amplitude and lifetime of magnetic fluctuations as the temperature approaches $T_C$ increases the random force acting on particles with spin located on the surface of a sample. This gives rise to an anomalous increase, in the vicinity of $T_C$, in the relaxation frequency of a particle governed by the dynamic correlation function of the random forces experienced by a particle with spin in a potential well and, in accordance with Ref. 1, creates a finite probability (proportional to the relaxation frequency) that such a particle will undergo a transition across a potential barrier.

We have detected such an anomalous behavior of the activated process of growth of oxide phase islands on the surface of nickel in the vicinity of the Curie point $T_C$ when the thickness of this phase is less than one monolayer. We found that the rate of formation of the oxide phase exhibits a maximum at the Curie point and a minimum in the ferromagnetic range of temperatures. Increasing the degree of coverage ($\theta > 0.6$) of the surface by oxide phase islands makes the singularities near $T_C$ disappear, and only a change in the activation energy of the process is observed in the transition across $T_C$.

Much work has been done on the interaction of oxygen with the surface of nickel (see, for example, the reviews in Refs. 2 and 3). It has been established that the formation of an oxide phase in the submonolayer range involves formation of nuclei and island growth. The only mechanism used so far to explain the growth of oxide phase islands on nickel[4] fails to account for the results we obtained near $T_C$. This is due to the assumption made in Ref. 4 that the rate of island growth is governed by the ratio of the frequencies of transition of adsorbed oxygen atoms from the same potential well to the oxide and gaseous (in the case of desorption) phases. According to Ref. 1, the temperature dependence of each of these frequencies has a singularity in the vicinity of $T_C$. However, the ratio of the frequencies of transitions to the oxide and gaseous phases does not have this singularity, which is in direct conflict with the experimental results (Fig. 7 below). We therefore carried out a systematic investigation of the interaction of oxygen with the surface of nickel in a wide range of temperatures in order to identify the mechanism of formation of the oxide phase during the island growth stage, so that we could describe all the experimental results.

We used (see Sec. II) the methods of low-energy ion scattering (LEIS), Auger electron spectroscopy (AES), and x-ray photoelectron spectroscopy (XPES). This made it possible to determine the density and state of the oxygen atoms on the surface of nickel and in a surface layer 10–15 Å deep. An increase in the exposure of the surface of nickel to oxygen, increasing the density of oxygen atoms in the chemisorbed state, transformed oxygen from this state to the oxide phase (in the form of islands with the NaCl-type structure) by "dropping" oxygen atoms to a subsurface state between the first and second layers of the surface atoms of nickel. In the case of oxygen atoms this state was intermediate between the chemisorbed and oxide phases. A collective process of transition of oxygen atoms from the chemisorbed to the subsurface state was predicted earlier[5] on the basis of a calculation of the binding energy of the oxygen atoms located in a nonuniform electron gas. An analysis of our experimental results led to the conclusion that an atom of oxygen in the subsurface state could either facilitate the displacement of a surface atom of nickel from its lattice site, followed by filling of the resultant vacancy (giving rise to an island of the oxide phase with the NaCl-type structure), or this oxygen atom could diffuse deeper into the sample.

The subsurface state of oxygen discovered in the present study was used in developing a mechanism of oxide phase formation on the surface of nickel capable of explaining all the experimental results (Sec. III). The oxide-island growth rate was governed by the probability $\omega$ for a surface atom of nickel to cross a potential barrier from a crystal lattice site of the metal to an oxide phase island. Participation of an atom of Ni (because of the exchange interaction with its neighbors) in the collective fluctuations of the spin subsystem of a magnetic material should result, according to Ref. 1, in an anomalous increase of the probability $\omega$ in the vicinity of the Curie temperature $T_C$ which would thus account for the singularities of the oxide phase growth in the vicinity of this temperature. The disappearance of these singularities on the surface coverage $\theta$ increases can be explained by the diffusion of oxygen atoms into the interior of the nickel sample, making it harder for long-wavelength spin waves to reach the surface layer. We shall show that the cutoff of the spec-

 0038-5646/89/040795-08$04.00  

trum of fluctuations of the magnetic moment of a magnetic material on the side of long wavelengths suppresses the divergence near $T_C$ of the relaxation frequency and, consequently, of the probability $\omega$, as indeed found by us experimentally.

## II. EXPERIMENTAL METHOD AND RESULTS

Our experiments were carried out using an XSAM-800 electron spectrometer with an energy resolution of 0.9 eV. We used the XPES, AES, and LEIS methods. The XPES and AES methods were capable of analyzing a surface layer of depth 10–15 Å; the LEIS method was capable of dealing only with the surface layer of atoms. We used x rays corresponding to the $K_\alpha$ transitions in Mg ($h\nu = 1253.6$ eV) and in Al ($h\nu = 1486.6$ eV). The binding energy of electrons was determined to within 0.1 eV. The energy spectra were calibrated using the $4f_{7/2}$ line of Au. It was found that formation of a thin (10–20 Å) oxide film did not alter the positions of the peaks in the XPES spectrum, i.e., the charging of the surface in our study of submonolayer coatings was negligible. In the LEIS experiments we determined the intensity of a beam of monoenergetic $He^+$ ions ($E = 1.5$ keV) scattered through an angle of 125° by the surface atoms of nickel.[6]

Our sample was a plate ($0.5\times0.6\times0.05$ cm) of polycrystalline nickel of at least 99.95% purity with the surface grains oriented mainly along (110). Before each measurement we cleaned the surface by several cycles consisting of bombardment with $Ar^+$ ions ($E = 2.5$ keV, current 2.5 $\mu$A/cm$^2$) and annealing in the presence of oxygen ($p = 10^{-6}$ torr) in order to remove carbon from the surface, followed by a second ion bombardment in order to remove the residual oxygen and annealing up to 700 K at a residual gas pressure of $10^{-10}$ torr. The AES measurements indicated that after this cleaning procedure the amounts of the impurities (carbon, oxygen, sulfur) remaining on the surface were near the sensitivity limit of the AES method and amounted to less than 0.01 monolayer. [In the case of the (110) surface of Ni one monolayer corresponded to a surface density $n_{\text{mon}} = 1.14\times10^{15}$ cm$^{-2}$.] During our experiments we did not detect any manifestations of the surface impurities. A sample was heated and its temperature was monitored using a special heater and a Chromel-Copel thermocouple. The temperature of a sample was kept constant to within $\Delta T/T \leqslant 0.5\%$ ($\Delta T \sim 3$ K). In the course of these experiments we studied the interaction of oxygen (of purity at least 99.95%) at pressures of $p = 10^{-6}$–$10^{-8}$ torr with the initially clean surface of Ni at temperatures 300–743 K. Oxygen was admitted directly into the chamber where the analysis was made and this chamber was pumped continuously.

We investigated possible states of oxygen atoms on the surface of nickel in the temperature range 500–743 K, which included the Curie point ($T_C = 631$ K). The photoelectron spectrum of oxygen included a line of intensity proportional to the number of oxygen atoms in the oxide. Figure 1a shows the 1$s$ spectra of O obtained after different exposures $\varepsilon$ ($\varepsilon = pt$, where $t$ is the duration of exposure) of the surface of a sample to oxygen at $T = 550$ K (the spectra obtained at other temperatures in the range 500–743 K were similar). These spectra were recorded after exposing a sample to oxygen, followed by shutting off the oxygen supply and pumping out the system to $10^{-9}$–$10^{-10}$ torr. In the range $\varepsilon < 40L$ ($1\ L = 10^{-6}$ torr·s) we observed a symmetric peak at $E_b = 530.5 \pm 0.1$ eV (spectrum 1 in Fig. 1a). We regarded this peak as symmetric if the wings of the line measured from its center to half-maximum were equal to within 5%. In the range $\varepsilon < 40L$ we found, as demonstrated in Fig. 1a (spectra 2, 3, and 4), that the left-hand wing of the line was more extended. For the sake of comparison, we included in Fig. 1a (spectrum 4) a calculated symmetric line of the same intensity. The $2p_{3/2}$ spectrum of Ni (Fig. 1b) obtained under the same conditions as the 1$s$ spectrum of O (1 in Fig. 1a) had two peaks with $E_b = 853.0 \pm 0.1$ eV and $E_b = 854.8 \pm 0.1$ eV. The former corresponded to nickel atoms in a metallic state.[7] The dashed curve in Fig. 1b shows, for the sake of comparison, the spectrum of pure nickel characterized by a peak at $E_b = 853.0$ eV. Experiments carried out using a standard sample of nickel oxide showed that the 1$s$ peak of O (530.5 eV) and $2p_{3/2}$ peak of Ni (854.8 eV) represented oxygen and nickel atoms in the oxide state, in agreement with the results of Ref. 7.

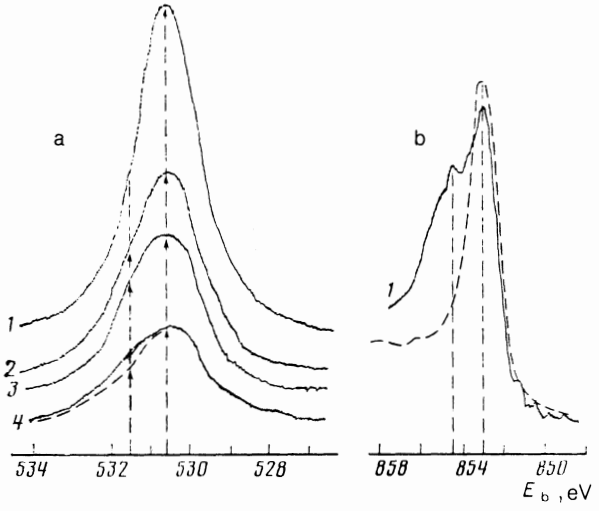


FIG. 1. Photoelectron spectra of the 1$s$ line of O (a) and $2p_{3/2}$ line of Ni (b) recorded at $T = 550$ K after different exposures $\varepsilon$: 1) $\varepsilon = 90L$;, 2) $40L$; 3) $20L$; 4) $2L$. The dashed line in Fig. 1a shows the $2p_{3/2}$ spectrum of Ni obtained for pure nickel (magnified by a factor of 3).

Sputtering of the surface layer by ion ($Ar^+$) bombardment removed the NiO monolayer formed as a result of an exposure $\varepsilon = 90L$ at $T = 550$ K (spectrum 1 in Fig. 1a), which destroyed the peak with $E_b = 530.5$ eV in the 1$s$ spectrum of O and gave rise to a peak at $E_b = 531.5$ eV (Fig. 2a). The resultant $2p_{3/2}$ spectrum of Ni (Fig. 2b) had a peak at $E_b = 853.0$ eV and corresponded to the spectrum of metallic nickel (dashed curve in Fig. 1b). Therefore, we could assume that the 1$s$ electrons of O with the binding energy $E_b = 531.5$ eV were due to oxygen atoms that diffused during growth of the NiO islands into the sample. Our analysis showed that the spectrum in Fig. 2a represented a signal from the oxygen atoms that diffused, in an amount representing 0.1 of a monolayer, into the surface layers (to a depth of the order of the mean free path of photoelectrons). Therefore, the asymmetry of the peak obtained after exposure in the range $\varepsilon < 40L$ (spectra 2–4 in Fig. 1a) could be explained by the presence of oxygen atoms that diffused into the interior of the sample and had a peak at $E_b = 531.5$ eV. The num-

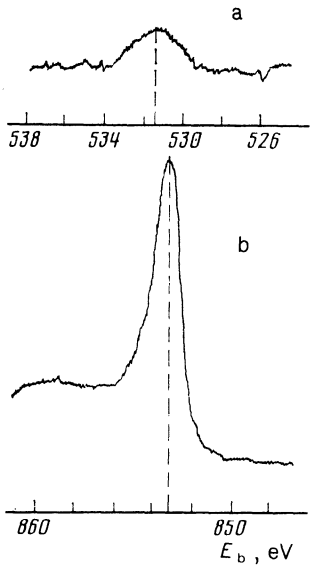


FIG. 2. Photoelectron spectra of the 1s line of O (a) and $2p_{3/2}$ line of Ni (b) after removal of a monolayer oxide film with ion bombardment at $T = 550$ K.

ber of oxygen atoms which diffused into the surface layer was proportional to the area in Fig. 1a between the dashed lines. The symmetry of the peak obtained at high exposures (spectrum 1 in Fig. 1a) could be due to the fact that, as the exposure increased, the contribution of the oxide state (peak at 530.5 eV) increased, whereas the number of diffused oxygen atoms remained constant and small.

A more detailed investigation of the diffusion of oxygen into a sample was made as follows. After short exposures of a sample to oxygen at $T = 300$ K the analyzer chamber was evacuated to $10^{-9}$–$10^{-10}$ torr. The resultant oxygen spectrum (1 in Fig. 3a) was asymmetric and had an intensity maximum at $E_b = 530.0 \pm 0.1$ eV. The $2p_{3/2}$ spectrum of Ni (Fig. 3b) obtained after such exposures had a peak at $E_b = 853.0$ eV, which was close to the spectrum of metallic nickel (dashed curve in Fig. 1b). We therefore assumed that the peak at $E_b = 530.0$ eV represented oxygen atoms in the chemisorbed state. As at temperatures in the range $T > 500$ K, the asymmetry of the peak (1 in Fig. 3a) was due to the presence of oxygen atoms which diffused into the interior of the sample (see the inset in Fig. 3a, where the two peaks at $E_b = 530.0$ and 531.5 eV are well resolved).[1)] The sample was then heated to a temperature in the range 400–700 K and maintained at this temperature for 15 min. This yielded the 1s spectrum of O (2 in Fig. 3a) with a peak at $E_b = 531.5$ eV and suppressed the peak at $E_b = 530.0$ eV. This indicated a reduction in the concentration of oxygen atoms on the surface and the presence of oxygen atoms dissolved in the surface layer. It was established that the activation energy of this process was $E_d \sim 0.6$ eV. Since the binding energy of the oxygen atoms on the surface of Ni was of the order of 5 eV (Ref. 8), the observed (Fig. 3) reduction in the surface density of oxygen could be attributed to the diffusion into the interior of the sample (and not due to desorption). The experiments reported in Ref. 9, in which the composition of the gaseous phase interacting with a single crystal of (100) Ni was monitored by mass spectrometry under conditions similar to ours, provided no evidence of desorption so that a reduction in the density of oxygen on the surface during heating was again attributed to the diffusion of oxygen into the interior of the sample.

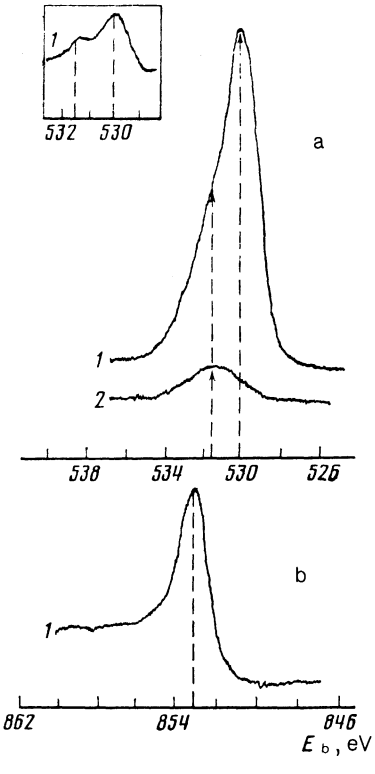


FIG. 3. Photoelectron spectra of the 1s line of O (a) and $2p_{3/2}$ line of Ni (b). The spectra labeled 1 were obtained at $T = 300$ K after an exposure of $\varepsilon = 30L$, whereas spectra labeled 2 were obtained after heating of an exposed sample for 15 min at $T = 600$ K. The inset shows the 1s spectrum of O obtained using $K_\alpha$ x rays from an Mg source.

The chemisorbed state of oxygen, characterized by the peak at $E_b = 530.0$ eV (spectrum 1 in Fig. 3a) dominating the contribution at $T \sim 300$ K, was not observed for $T > 500$ K for any exposure. Since in the spectra in Fig. 1a the main peak at $E_b = 530.5$ eV had a strong shoulder on the side of high binding energies (due to the contribution of the peak with $E_b = 531.5$ eV), we concluded that the chemisorbed oxygen (if present at all on the surface at such temperatures) gave rise to the 1s signal of O, which was at least less than that of the dissolved oxygen. The oxygen spectra we obtained were in good agreement with those reported in Ref. 10, where the XPES method was used at $T > 500$ K to detect only the oxide state of oxygen (with a peak at $E_b = 530.4$ eV) on the surface of polycrystalline nickel.

As pointed out above (Fig. 3a), small exposures ($\varepsilon \leqslant 40L$) at room temperature revealed only the oxygen lines in the chemisorbed and dissolved states (see also spectra 1–3 in Fig. 4a). An increase in the exposure ($\varepsilon > 40L$) shifted the intensity maximum in the 1s spectrum of O toward $E_b = 530.5$ eV (spectrum 4 in Fig. 4a). The left-hand wing of the $2p_{3/2}$ line of Ni (Fig. 4b) became extended compared with the spectrum of pure nickel. These observations indicated formation of nickel oxide on the surface. When NiO was formed the 1s spectrum of O (spectrum 4 in Fig. 4a) observed at $T = 300$ K included contributions of all three peaks (530.0, 530.5, and 531.5 eV); we were unable to determine accurately the quantitative relationships between these peaks without a suitable mathematical procedure. However, this was unnecessary in our study of the growth of

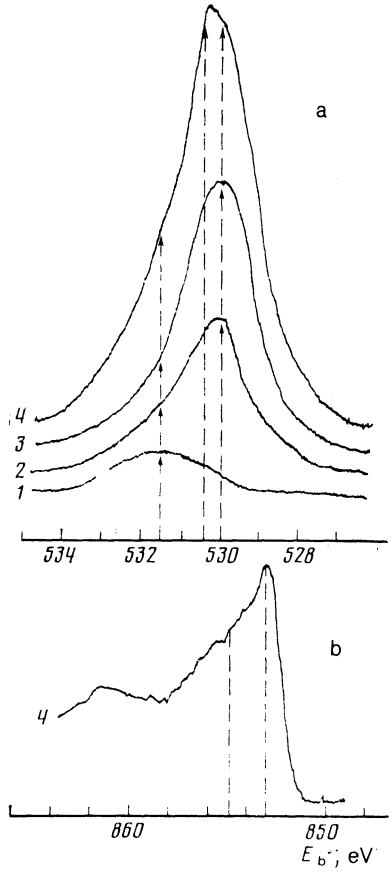


FIG. 4. Photoelectron spectra of the 1s line of O (a) and $2p_{3/2}$ line of Ni (b) recorded at $T = 300$ K after different exposures $\varepsilon$: 1) $\varepsilon = 2L$; 2) $20L$; 3) $40L$; 4) $90L$.

the oxide phase in the vicinity of $T_C$, because at temperatures $T > 500$ K the relative contribution of the states with $E_b = 530.0$ and 531.5 eV to the measured signal of oxygen in the oxide (530.5 eV) was slight (0.1 monolayer), as demonstrated above, and it decreased on the exposure increased.

Changes in the state of the surface of nickel due to its interaction with oxygen were also investigated by the low energy ion scattering (LEIS) method. Figure 5 shows the dependence of the relative intensity $i$, representing the ions scattered by surface Ni atoms, on the exposure $\varepsilon$ at $T = 300$ K. The value of $i$ was proportional to the density of the scattering atoms[11,12] (i.e., to the density $n_s$ of the Ni atoms on the surface). The observed (Fig. 5) reduction in the value of $i$ (and, consequently, in the value of $n_s$) in the range $\varepsilon < 30L$

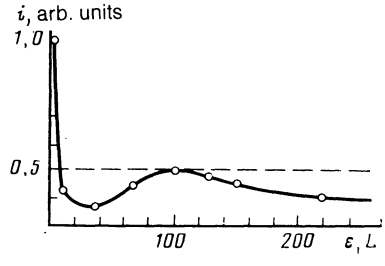


FIG. 5. Dependence of the relative intensity of the flux of scattered ions $i$ on the exposure $\varepsilon$ ($i = I_e / I_0$, where $I_0$ and $I_e$ are the intensities of the ions scattered by the surface nickel atoms in the case of clean and oxygen-exposed surfaces, respectively).

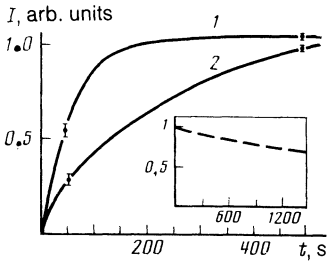


FIG. 6. Dependence of the intensity $I$ of 1s photoelectron peak of O at 530.5 eV on the duration of exposure $t$ at various temperatures: 1) 513 K; 2) 743 K. The inset shows (dashed curve) the kinetics of dissociation (at $T = 513$ K and $p = 10^{-9}$ torr) of a monolayer oxide film formed at $T = 300$ K.

could be explained by the fact that the surface atoms of nickel were in the shadow of the oxygen atoms in the chemisorbed state. Two characteristic features of the dependence in Fig. 5 should be noted. In the range $\varepsilon = (30\text{–}100)L$ an increase in the exposure increased the value of $i$, indicating an increase in $n_s$. In the range $\varepsilon > 200L$, when the surface of the sample carried a monolayer oxide film, the value of $i$ tended to the saturation limit $i_{sat} = 0.41 \pm 0.02$. At $T > 500$ K this limit was $i_{sat} = 0.50 \pm 0.02$ (Ref. 6). Since the value of $i_{sat}$ was close to 1/2, typical of NiO with the NaCl-type structure, we concluded that the resultant oxide had the NaCl-type structure. This was supported by the results of Refs. 13 and 14 where the methods of high-energy electron diffraction and photoelectron diffraction were used to show that a monolayer oxide film formed on the surface under conditions similar to ours had the NaCl-type structure. A reduction in the value of $i$ compared with 1/2 at $T = 300$ K could be explained by additional "shadowing" of the nickel atoms by the chemisorbed oxygen on top of the NiO film. The results of the experiments carried out using the LEIS method were in good agreement with those reported above and obtained by the XPES method.

We investigated the rate of formation of oxide on the surface of a sample at a fixed temperature by recording how the intensity $I$, defined as the amplitude of the 1s peak of O representing photoelectrons with $E_b = 530.5$ eV, depended on the duration of exposure $t$ of the surface of Ni to oxygen. Figure 6 reproduces $I(t)$ curves recorded at two temperatures (513 and 743 K) at an oxygen pressure of $p = 10^{-6}$ torr employing an $X$-$Y$ plotter. Since the peak with $E_b = 530.5 \pm 0.1$ eV corresponded at these temperatures principally to the atoms of oxygen in the oxide state, the curves in Fig. 6 represent the kinetic dependence of the formation of the oxide phase on the surface of nickel. The accuracy with which the amount of oxygen in NiO could be determined depended on the characteristics of the apparatus and on the contribution of the dissolved oxygen: it amounted to 5% but improved to 2% in the range $\varepsilon > 200L$. With increasing $t$ the value of $I$ tended to approach the saturation limit $I_{sat}$ (curve 1 in Fig. 6). Since the room-temperature value of $I_{sat}$ corresponded to a monolayer coating of the surface by nickel oxide,[4] the degree of coverage $\theta$ of the surface of a nickel sample by the oxide phase was defined as the ratio

$$\theta = I/I_{sat},$$

where $I_{sat}$ is the intensity of the 1s peak of O observed on

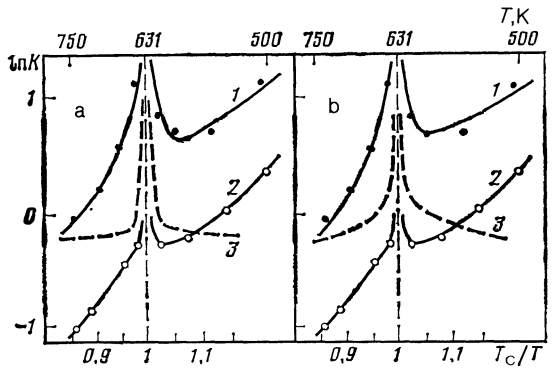


FIG. 7. Dependence of the rate of formation $K$ of the oxide phase on the reciprocal of temperature plotted for $\theta = 0.25$ (1) and 0.6 (2). The solid curves represent the theoretical dependence of Eq. (15) obtained using a model of magnetic material with conserved (a) and nonconserved (b) spin and assuming the following parameters: $\gamma = 0.9$ $A_1' = 2\times10^{-3}$, $A_2'$ $= 0.13$ (curve 1); $\gamma = 2.2$, $A_1' = 1\times10^{-3}$, $A_2' = 0.04$ (curve 2); $E_V^0/T_C$ $= 5$, $E_d/T_C = 9.5$. The dashed curve (3) represents the dependence of the logarithm of the relaxation frequency $\eta$ on the reciprocal of temperature in the case when $\rho = 0.25$.

saturation at room temperature. It is clear from Fig. 6 that in the range $\theta = 0.5$–1 an increase in temperature reduced the rate of formation of the oxide phase $K \approx (dI/dt)|_I$. A comparison of the dependences represented by dashed and solid curves in Fig. 6 indicated that the characteristic oxide formation time was an order of magnitude less than the oxide dissociation time at the same temperature. Consequently, we could ignore the dissociation of oxide under our experimental conditions.

Figure 7 shows the dependence of the oxide formation rate $K$ on the sample temperature when the surface coverage was $\theta = 0.25$ or 0.6. For $\theta = 0.25$ there was a maximum near the Curie point and a minimum in the ferromagnetic range of temperatures. An increase in $\theta$ to 0.6 destroyed these singularities. Far from $T_C$, when the surface coverage was $\theta = 0.25$ or 0.6, the rate of formation of the oxide phase $K$ regarded as a function of temperature could be described by the following relationship (accurate to within experimental error):

$$K = K_0 \exp(-E_a/T),$$

where $E_a$ is a constant (with the dimensions of energy), which was different on different sides of $T_C$. The dependence of the value of $E_a$ on the coverage of the nickel surface with the oxide phase in the ferromagnetic and paramagnetic states of the sample was also determined (Fig. 8). Clearly, the value of $E_a$ increased with the degree of surface coverage. The difference between these energies in the ferromagnetic and paramagnetic states $\Delta E_a = E_a^f - E_a^p$ was 0.22 eV, which was independent of $\theta$.

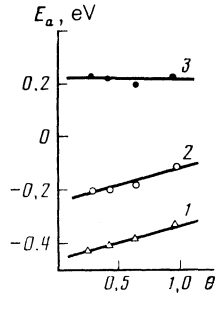


FIG. 8. Dependences of the values of $E_a$ (1,2) and of the difference between the energies $\Delta E_a$ (3) on the surface coverage $\theta$ in the paramagnetic (1) and ferromagnetic (2) states of a sample.

## III. DISCUSSION

During the initial stage of the interaction between nickel and oxygen (corresponding to low surface coverages) the atoms of oxygen were in a chemisorbed state at $T = 300$ K (Sec. II). An increase in the density of oxygen atoms in the chemisorbed state $n_{cs}$ generated nickel oxide beginning from $n_{cs} > 7\times10^{14}$ cm$^{-2}$ ($\theta > 0.62$). This value was deduced from the position of the minimum of the dependence $i = f(\varepsilon)$ (Fig. 5), which could be explained by completion of the stage of chemisorption at the onset of oxide formation. It was shown in Refs. 4 and 13 that the chemisorbed and oxide phases coexisted in the course of oxide formation. At temperatures in the range 310–570 K it was found[13] that the average size of an oxide-phase island was several tens of angstroms. The oxide-phase islands were observed directly (by electron spectroscopy)[15] on the surface of nickel for $T > 500$ K. Therefore, there were grounds for assuming that in the range of temperatures under consideration the transition of the oxygen atoms from the chemisorbed to the oxide state was a first-order phase transition.

Formation of a new phase as a result of a first-order transition is known to involve nucleation and island growth.[16] We shall derive the time and temperature dependences [see Eq. (9) below] of the degree of coverage $\theta$ of the sample surface by oxide-phase islands using the following very simple model (Fig. 9). We assume initial instantaneous formation of growth nuclei at centers distributed at random on the surface and characterized by a density $N_0$. For the sake of simplicity, we assume that new islands grow in isolation from one another in the form of disks. An island which forms at a nucleation center grows as follows (Fig. 9). A chemisorbed oxygen atom at the perimeter of an island can go over to the subsurface state with the probability

$$\alpha = \alpha_0 \exp[-Q/T]$$

(see Fig. 9). Here, $Q = 0.41$ eV is the height of the potential barrier[5] separating the chemisorbed and subsurface states of oxygen. An increase in the value of $i$ in the range $\varepsilon = (30$–$100)L$ after completion of the chemisorption stage (Fig. 5) can be explained by the dropping of oxygen atoms to the subsurface state. A comparison of the dependence $i = f(\varepsilon)$ in Fig. 5 with the corresponding dependence exhibited by the XPES signal at $T = 300$ K shows that the oxygen atoms

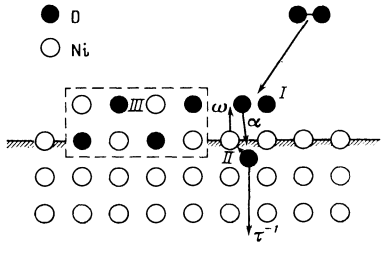


FIG. 9. Schematic representation of a model of growth of an oxide phase on the surface of nickel. The dashed line surrounds an island of NiO; I, II, and III are the chemisorbed, subsurface, and oxide states of oxygen, respectively.

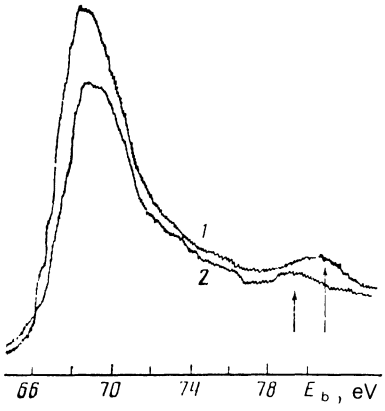


FIG. 10. Photoelectron spectra of the 3$p$ line of Ni obtained for clean nickel (1) and after exposure to oxygen at $T = 300$ K (2). The arrows identify the plasmon satellites representing double excitation of plasmons by the emitted photoelectrons.

dropping to the subsurface state are localized in a surface layer less than 5 Å thick. This process reduces the electron density $n_0$ in nickel, so that the system energy decreases.[5] We deduced the reduction in $n_0$ by a factor of 1.21 while the oxygen and nickel interacted from the reduction in the plasmon frequency

$$\omega_p = (4\pi n_0 e^2/m_e)^{1/2},$$

deduced from the position of the peak of the plasmon satellite in the 3$p$ spectrum of Ni (Fig. 10). The dropping of oxygen to the subsurface state can clearly account for the change in the sign of the dipole moment of surface layers at the island growth stage, as deduced from the experimentally determined work function of electrons.[4] An atom of oxygen in the subsurface state at an interstice can displace the nearest surface Ni atom from its lattice site (Fig. 9) and thus create a vacancy; the frequency of this process is

$$\omega = \omega_0 \exp(-E_V/T), \tag{1}$$

where $E_V$ is the depth of the potential well in which a surface nickel atom is located at a lattice site.

The attachment of a subsurface oxygen atom to an oxide-phase island involves filling a vacancy formed in this way in a time interval $t_f \ll \omega^{-1}$. The frequency of formation of the oxide particles is then described by Eq. (1). An oxygen atom located in the initial chemisorbed state near an atom that has gone over to the subsurface state becomes bound to a nickel atom displaced from a lattice site and it remains on the surface (Fig. 9). The island structure with alternate oxygen and nickel atoms at the lattice sites, formed as a result of this "musical chairs" effect is that of the nickel oxide (of the NaCl type). In addition to a transition to the oxide, a subsurface oxygen atom can diffuse deeper into the sample. The probability of this process is $\tau^{-1}$, with

$$\tau = \tau_0 \exp(E_d/T), \tag{2}$$

where $E_d$ is the activation energy of the diffusion of oxygen into the interior of a sample.

The changes in the relative concentrations of oxygen $\theta_i n_i/n_{ms}$ in the chemisorbed ($\theta_{cs}$), subsurface ($\theta_{ss}$), and oxide ($\theta_{ox}$) states is described by the following system of rate equations:

$$\begin{aligned} \dot\theta_{cs} &= J\sigma(1-\theta_{cs}) - \alpha\theta_{cs}, \\ \dot\theta_{ss} &= \alpha\theta_{xc} - \omega\theta_{ss} - \theta_{ss}\tau^{-1}, \\ \dot\theta_{ox} &= \omega\theta_{ss}. \end{aligned} \tag{3}$$

Here, $J$ is the flux of molecules to the surface and $\sigma$ is the cross section of an oxygen molecule. The system of equations (3) allows for the fact that we can ignore the desorption of chemisorbed oxygen and the dissociation of the oxide under the experimental conditions (see Sec. II). The rate of growth of the oxide-phase island cannot be governed by the surface diffusion of chemisorbed oxygen, because the diffusion length $l_d$ is short in the investigated temperature range:

$$l_d = (D_s\alpha^{-1})^{1/2} \lesssim 10^{-8}\ \text{cm};\ D_s = a^2\nu \exp(-E_s/T)$$
$$(a \approx 5\ \text{Å}, \nu = 10^{13}\ \text{s}^{-1}, E_s \approx 1\ \text{eV}, \alpha_0 \approx 10^{13}\ \text{s}^{-1},$$
$$Q = 0.41\ \text{eV}).$$

Since according to Eq. (3), the characteristic time of formation of the oxide phase $\tau_{ox} = \omega^{-1}$ is much longer than the characteristic times $\tau_{ss}(\omega + \tau^{-1})^{-1}$ and $\tau_{cs} = (\alpha + J\sigma)^{-1}$ (the inequality $\tau_{ox} \gg \tau_{cs}$ follows from the fact that the chemisorbed oxygen is not observed at temperatures $T > 500$ K—see Sec. II), we shall consider a quasisteady state of the system ($\dot\theta_{cs} = 0$, $\dot\theta_{ss} = 0$). Then, the change in the oxygen concentration in one oxide-phase island is given by the expression

$$\dot\theta_{ox} = \frac{\alpha J\sigma\omega\tau}{(J\sigma+\alpha)(\omega\tau+1)}. \tag{4}$$

As pointed out above, the steady-state value of the density of the chemisorbed oxygen under the experimental conditions is $\theta_{cs}^s \ll 1$. It then follows from Eq. (3) that the inequality $\alpha \gg J\sigma$, is obeyed and Eq. (4) yields

$$\dot\theta_{ox} = \frac{J\sigma\omega\tau}{\omega\tau+1}. \tag{5}$$

The rate of increase in the island radius $R$ is related to the change in the oxygen density in the oxide state [Eq. (5)] by

$$\dot R = \dot\theta_{ox}\sigma^{1/2}. \tag{6}$$

We can see that the radial growth rate $\dot R$ of an oxide-phase island is independent of time. This is a consequence of failing to allow for dissociation of the oxide in the system of equations (3). The rate of dissociation of the oxide is low, compared with the rate of attachment of oxygen atoms to an oxide-phase island, which is equivalent to the conclusion that the critical size of the growth nuclei $R_c$ is small. As shown in Ref. 17, the rate of growth of the nuclei in the case of a first-order phase transition is given by the expression

$$\dot R \propto \left(\frac{1}{R_c} - \frac{1}{R}\right). \tag{7}$$

Then, if $R \gg R_c$, the radial growth rate is constant. Substitution of Eq. (5) in Eq. (6) gives the following expression for the radius of an island

$$R(t) = J\sigma^{1/2}\frac{\omega\tau}{\omega\tau+1}t. \tag{8}$$

The coverage $\theta$ of the surface by islands of the new phase, deduced using the phenomenological approach in Refs. 18 and 19, is given by

$$\theta=1-\exp[-\pi R^2(t)N_0].$$

Using Eq. (8), we obtain

$$\theta=1-\exp[-(t/t^*)^2], \tag{9}$$

where

$$t^*=\frac{1+\omega\tau}{(\pi N_0)^{1/2}J\sigma^{3/2}\omega\tau} \tag{10}$$

represents the average island coalescence time. Using Eq. (9) and allowing for Eqs. (1) and (2), we find that the surface coverage $\theta(t)$ and the rate of formation of the oxide phase $K=(d\theta/dt)|_\theta$ depend on temperature only if $\omega\tau\lesssim 1$. Since the observed dependences $\theta(t)$ (Fig. 6) and $K(T)$ (Fig. 7) are different at different temperatures, the description of the experimental data on the basis of Eq. (9) is possible only if $\omega\tau\lesssim 1$. (The estimates given below indicate that under experimental conditions we have $\omega\tau\lesssim 10^{-1}$.) It then follows from Eq. (9) that the rate of formation of the oxide phase is

$$K=C\omega_0\exp\left(-\frac{E_V-E_d}{T}\right). \tag{11}$$

A comparison of the experimental data with Eqs. (11) and (9) allows us to conclude that the proposed model of formation of the oxide phase on the surface of nickel describes satisfactorily the experimental data far from $T_C$. Firstly, Eq. (9) describes, within the limits of the experimental error, the dependence shown in Fig. 6 within the range $\theta=0.5$–1. Secondly, the observed exponential reduction in the rate of formation of NiO as a function of temperature (Fig. 6, straight lines far from $T_C$ in Fig. 7) can indeed be described by the relationship (11), since $E_d\approx 0.6$ eV is greater than $E_V\approx 0.3$ eV (Ref. 20). The difference between the activation energies $E_d-E_V\approx -0.3$ eV is close to the experimentally determined value of $E_a$ (Fig. 8).

We can explain the anomalous behavior of the rate of formation of the oxide phase near $T_C$ (Fig. 7) using the results of Ref. 1. An expression was obtained in Ref. 1 for the probability that a particle with a spin would emerge from a potential well under the influence of fluctuations of the magnetic moment of nickel. As shown above, the formation of NiO involves the transfer of a nickel atom from one stable (metallic) to another stable (oxide) state. The exchange interaction with the neighbors results in their participation in collective fluctuations in nickel. According to Ref. 1, the probability $\omega$ that a particle (Ni atom) is displaced from a potential well by random forces due to fluctuations of the thermostat (representing the electron, phonon, and spin subsystems) is given by the expression

$$\omega=\eta\frac{E_V}{T}\exp\left(-\frac{E_V}{T}\right), \quad \text{i.e.,} \quad \omega_0\equiv\eta\frac{E_V}{T}. \tag{12}$$

The relaxation frequency $\eta$ of a nickel atom is

$$\eta=\eta_e+\eta_{ph}+\eta_{sp},$$

where $\eta_e$, $\eta_{ph}$, and $\eta_{sp}$ are tne relaxation frequencies of an atom of nickel interacting with the electron, phonon, and spin subsystems, respectively. Since the validity of the models of critical dynamics in the description of the magnetic properties of Ni is not yet certain, the value of $\eta_{sp}$ was calculated using models in which spin is conserved or not conserved. The relaxation frequency $\eta_{sp}$ is then of the form

$$\eta_{sp}^i=A_i\frac{\xi^{p_i}}{T}. \tag{13}$$

Here, $p_1=3$ in a model of a magnetic material with a conserved spin and $p_2=1$ in a model with a nonconserved spin; $\xi^\alpha|T_C-T|^{-1/2}$ is the correlation length of the magnetic material and $A_i$ is a constant independent of temperature. In contrast to $\eta_{sp}$, the relaxation frequencies $\eta_e$ and $\eta_{ph}$ do not have a singularity near $T_C$. The energy $E_V$ is given by[1]

$$\frac{E_V}{T}=\frac{E_V^0}{T_C}x+\gamma[(x^2-x)\tilde{\theta}(x-1)]^{1/2}, \tag{14}$$

where $E_V^0$ is the potential barrier due to the interaction of a particle with the electron subsystem; $\gamma$ is a quantity proportional to the exchange interaction energy $W$ of the magnetic material; $x=T_C/T$; $\tilde{\theta}(x-1)$ is the Heaviside function.

The expression for the rate of formation of the oxide phase [Eq. (11)] can be represented as follows in the vicinity of $T_C$ if we use Eqs. (12) and (13):

$$\ln K=\ln C'+\ln\left(1+A_i'\frac{\xi^{p_i}}{T}\right)+\ln\frac{E_V}{T}-\frac{E_V}{T}+\frac{E_d}{T}, \tag{15}$$

where

$$C'=C(\eta_e+\eta_{ph}),\ A_i'=A_i/(\eta_e+\eta_{ph}).$$

The values of $K$ calculated from Eq. (15) are represented by solid traces in Fig. 7. We can see that the calculated dependences agree (to within the limits of experimental error) with the results of our experiments. The existence of a maximum in the rate of formation of the oxide phase in the limit $T\to T_C$ and a minimum in the ferromagnetic range of temperatures is explained—in accordance with Eqs. (15) and (13)—by an increase in the frequency of relaxation of a nickel atom as the temperature approaches $T_C$ (dashed curve in Fig. 7). This occurs because of an increase in the random force exerted on a nickel atom by the spin subsystem, and because of an increase in the duration of its action on a particle in the limit $T\to T_C$.

The different slopes on the rectilinear parts of the dependence $\ln K=f(T^{-1})$ far from $T_C$ (Fig. 7) and the consequently different activation energies $E_a$ (Fig. 8) in the paramagnetic and ferromagnetic states are due to, according to Eq. (14), the influence of the exchange interaction of a magnetic material on the height of the barrier $E_V$ that has to be overcome by a nickel atom in the course of its displacement from a lattice site (i.e., $E_V^f-E_V^p=W$). The experimentally obtained difference $\Delta E_a=0.22$ eV between the activation energies is in good agreement with the exchange interaction energy $W=0.25$ eV given in the literature.[21,22]

Equation (12) used to describe the experimental data in the vicinity of $T_C$ is valid for $\eta<\Omega T/E_V$ (Ref. 1); here, $\Omega$ is the characteristic frequency of motion of a particle ($\Omega\sim\omega_D$, where $\omega_D$ is the Debye frequency, which in the case of Ni amounts to $\approx 6\times 10^{13}$ s$^{-1}$—see Ref. 23). We now show that

this inequality is indeed satisfied. If we use Eqs. (1), (2), and (12), it follows from Eq. (10) that

$$\eta = \frac{1}{(\pi N_0)^{1/2} J \sigma^{1/2} t^* \tau_0} \frac{T}{E_V} \exp[(E_V - E_d)/T]. \quad (16)$$

In our estimates we assume that $N_0 \sim 10^{11}\,\mathrm{cm}^{-2}$, which is the density of defects on the surface, $J = p/(2\pi m T_g)^{1/2}$, $T_g = 300\,\mathrm{K}$, $p = 10^{-6}\,\mathrm{Torr}$, $\sigma \sim 10^{-15}\,\mathrm{cm}^2$, $\tau_0 \sim 10^{-13}\,\mathrm{s}$, $E_V = 0.3$ eV, $E_V - E_d = -0.2$ eV. The experimental results obtained at $T = 600$ K give $t^* \sim 25$ s. It then follows from Eq. (16) that

$$\eta \approx 7 \cdot 10^9\,\mathrm{s}^{-1} \ll \Omega \frac{T}{E_V} \approx 10^{13}\,\mathrm{s}^{-1}.$$

Using the relaxation frequency $\eta$ of a nickel atom, we find that—as assumed in the derivation of Eq. (11)—the following inequality is satisfied:

$$\omega\tau = \eta \frac{E_V}{T} \tau_0 \exp[(E_d - E_V)/T] \approx 10^{-1} \ll 1.$$

An increase in the surface coverage $\theta$ flattens out the singularities of the rate of formation of the oxide phase in the vicinity of $T_C$ (Fig. 7), which can be explained as follows. As shown in Sec. II, oxygen diffuses into the interior of a sample as NiO islands grow. For example, for $T \approx 600$ K at the moment when $\theta = 0.6$ is reached, a surface layer with thickness of the order of the diffusion length $L_d$ ($L_d \sim 10^{-3}$ cm at $T = 600$ K when $t = 100$ s) contains $n_d \approx 5 \times 10^{19}\,\mathrm{cm}^{-3}$ of oxygen atoms which diffused. A local perturbation of the nearest Ni atoms by an oxygen atom located at an interstice inside a sample may suppress the appearance in the surface layer, of spin waves of wavelength $\lambda_{\max} \propto (n_d)^{-1/3}$, greater than the average distance between the oxygen atoms. An increase in the number of oxygen atoms in the interior of a sample (and, consequently, on increase in $\theta$) reduces $\lambda_{\max}$ and, consequently, the wave vector $k_0 = 2\pi/\lambda_{\max}$ increases ($\partial k_0/\partial\theta > 0$). Then, calculating again the relaxation frequency $n_{sp}$, but allowing for the limitations on the wave vector, we find (in agreement with Ref. 1) that

$$\eta_{sp}^{\,i} = A_i'' \frac{\xi^{pi}}{T}\left[\frac{\pi}{4} - \frac{1}{2}\operatorname{arctg}(k_0\xi) + (-1)^i \frac{k_0\xi}{2(1+(k_0\xi))^2}\right] \quad (17)$$

($A_i''\pi/4 = A_i$). It should be noted that in the limit $k_0 \to 0$ ($\theta \to 0$), Eq. (17) reduces to Eq. (13).

The dependence of the rate of formation of the oxide phase in the vicinity of $T_C$ obtained allowing for Eq. (17) describes the experimental results well (Fig. 7). It readily follows from Eq. (17) that $\partial\eta_{sp}/\partial\theta < 0$, i.e., that the relaxation frequency of a particle and, consequently—according to Eq. (12)—the probability of displacement of a nickel atom from a potential well decreases as $\theta$ increases. When a certain critical value $\theta_C$ is reached, calculations based on Eq. (17) show that the singularities exhibited at $T = T_C$ by the dependence $\eta_{sp} = f(T^{-1})$ and $\omega = f(T)^{-1}$ disappear. Therefore, the observed (Fig. 7) reduction and disappearance of fluctuation-induced singularities in the rate of growth of the oxide phase with increasing $\theta$ can be explained by a reduction in the relaxation frequency $\eta_{sp}$ caused by damping of long-wavelength spin waves because of the diffusion of oxygen atoms into the interior of a sample.

[1)]The use of an Mg x-ray source ensured a high spectral resolution, but it was difficult to employ this source in a quantitative analysis because in the investigated range of energies (corresponding to the 1*s* line of O) nickel has an Auger peak. Therefore, all the spectra, except that shown in the inset of Fig. 3a, were obtained using an Al source.


[1]V. D. Borman, A. N. Pivovarov, and V. I. Troyan, Pis'ma Zh. Eksp. Teor. Fiz. **39**, 458 (1984) [JETP Lett. **39**, 556 (1984)].
[2]A. Atkinson, Rev. Mod. Phys. **57**, 437 (1985).
[3]P. H. Holloway, J. Vac. Sci. Technol. **18**, 653 (1981).
[4]P. H. Holloway and J. B. Hudson, Surf. Sci. **43**, 123 (1974).
[5]B. Chakraborty, S. Holloway, and J. K. Norskov, Surf. Sci. **152–153**, 660 (1985).
[6]V. D. Borman, E. P. Gusev, Yu. Yu. Lebedinskiĭ, and V. I. Troyan, Poverkhnost' No. 11, 138 (1988).
[7]K. Wandelt, Surf. Sci. Rep. **2**, 1 (1982).
[8]I. Toyoshima and G. A. Somorjai, Catal. Rev. Sci. Eng. **19**, 105 (1979).
[9]A. R. Kortan and R. L. Park, Phys. Rev. B **23**, 6340 (1981).
[10]G. C. Allen, P. M. Tucker, and R. Wild, Oxidat. Met. **13**, 223 (1979).
[11]V. A. Kurnaev, E. S. Mashkova, and V. A. Molchanov, *Reflection of Light Ions from the Surface of a Solid* [in Russian], Énergoatomizdat, Moscow (1985).
[12]M. I. Ryazanov and I. S. Tilinin, *Surface Investigations Using Particle Backscattering* [in Russian], Énergoatomizdat, Moscow (1985).
[13]D. F. Mitchell, P. B. Sewell, and M. Cohen, Surf. Sci. **69**, 310 (1977).
[14]R. Saiki, A. Kaduwela, J. Osterwalder, *et al.*, J. Vac. Sci. Technol. A **5**, 932 (1987).
[15]K. R. Lawless, in: *Energetics in Metallurgical Phenomena, Vol. 1* (ed. by W. M. Mueller), Gordon and Breach, New York (1965), p. 345.
[16]L. D. Landau and E. M. Lifshitz, *Statistical Physics, Vol. 1*, 3rd ed., Pergamon Press, Oxford (1980).
[17]A. Z. Patashinskiĭ and B. I. Shumilo, Zh. Eksp. Teor. Fiz. **77**, 1417 (1979) [Sov. Phys. JETP **50**, 712 (1979)].
[18]A. N. Kolmogorov, Izv. Akad. Nauk SSSR Ser. Mat. No. 3, 355 (1937).
[19]V. Z. Belen'kiĭ, *Geometric--Probabilistic Models of Crystallization* [in Russian], Nauka, Moscow (1980), p. 13.
[20]R. J. Behm, G. Ertl, and J. Wintterlin, Ber. Bunsenges. Phys. Chem. **90**, 294 (1986).
[21]W. Schmitt, K. P. Kämper, and G. Guntherodt, Phys. Rev. B **36**, 3763 (1987).
[22]G. T. Rado and H. Suhl (eds.), in: *Magnetism: A Treatise on Modern Theory and Materials, Vol. 4*, Academic Press, New York (1966), p. 123.
[23]C. Kittel, *Introduction to Solid State Physics*, 2nd ed., Wiley, New York (1956).


Translated by A. Tybulewicz